Desalination and Water Treatment
www.deswater.com

doi: 10.5004/dwt.2020.25961

197 (2020) 182–190
September

Ex-situ synthesis of bacterial cellulose-copper oxide nanoparticles for effective chemical and biological properties

Yasir Anwar[a,b,*], Ihsan Ullah[a], Majed A. Al-Shaeri[a,b], Bassam Oudh AlJohny[a]

[a]*Department of Biological Sciences, Faculty of Science, King Abdulaziz University, Saudi Arabia, emails: yanwarulhaq@kau.edu.sa/ yasirpcsir2006@gmail.com (Y. Anwar), ihsanknu@gmail.com (I. Ullah), malshaere@kau.edu.sa (M.A. Al-Shaeri), aljohnybassam@gmail.com (B.O. AlJohny)*
[b]*Princess Dr. Najla Bint Saud Al-Saud Center for Excellence Research in Biotechnology, King Abdulaziz University, Saudi Arabia*

Received 13 October 2019; Accepted 10 April 2020

ABSTRACT

Bacterial cellulose (BC), an important biopolymer has received a tremendous application in biomedical and other related fields. Herein, we have tried to cope with its deficiency of lacking bactericidal features via impregnating copper oxide nanoparticles (CuO NPs) in the BC matrix. BC-CuO composites were synthesized through an *ex-situ* composite synthesis strategy and were validated with several analytical tools. Dry weight analysis confirmed 35% NPs attachment in composites while the observed slow release behavior augmented their stability. Field emission–scanning electron microscopy and X-ray diffraction analysis provided a clear view of NPs attachment to the BC surface fibrils and its deep penetration in the matrix. The composite material was tested for two applications. It was noteworthy that synthesized BC-CuO composites provided impressive antibacterial activities against both *Escherichia coli* and *S. aureus* and reduced their growth to 96% and 87%, respectively. Moreover, the composite was also used for the treatment of the wastewater as revealed by testing it against simulated wastewater containing Methyl Orange dye. The bactericidal, nontoxic, and catalytic behavior of BC-CuO composites can provide insight for potential biomedical and environmental applications.

Keywords: Antibacterial; CuO; Nanoparticles; Bacterial cellulose; Methyl Orange; Reduction reaction

1. Introduction

Bacterial cellulose (BC), one of the important bioproduct, is produced by a certain class of bacteria [1]. The chemical structure of BC is similar to that of plant cellulose, however, it has much better physical, mechanical, and biological properties thanks to its high purity, crystallinity, and porous nanofibril network structure [2]. BC has received applications in diversified fields, more prominently in wound healing, facial masks development, antimicrobial membranes, skin tissue repair, drug delivery, electronic, display devices, diaphragms, foods, and paper industry [3]. Regardless of its impressive features, as a matter of fact, BC lacks antimicrobial properties and biodegradability. These shortcomings greatly affect its application to some extent especially if BC is used as dressing material as wound healing in an infected environment and as a bactericidal filter etc.

Nanomaterials have been widely utilized in various fields including medical, conducting materials, catalysis, filtration, etc. due to their high surface energy and large surface area and antimicrobial characteristics [4–7]. Earlier, some nanomaterials like, silver, zinc oxide, titanium oxide,

* Corresponding author.

nickel oxide, and clay materials have been utilized in various bio-composites for impregnating bactericidal features [2,8]. Furthermore, nanomaterials have been utilized for adding conducting, catalytic and magnetic properties to various polymers [9–12]. However costly nature and complex synthetic strategies might reduce the efficacy of nanomaterials in composite synthesis and large scale applications [5,13–16]. Copper oxide (CuO), in this regard, could be cheaper and simple alternative to noble metals such as gold and silver nanoparticles. It is a typical *p*-type semiconductor that has been vastly used in catalytic, batteries-related, sensors, and antimicrobial studies [17]. While using the nanoparticles of CuO as a catalyst, a common problem of aggregation is faced. Moreover, such small nanoparticles could not be separated for re-use. Therefore, a study concerning the effective use of the CuO as a catalyst while avoiding their aggregation is highly desirable.

A major drawback presently associated with BC is its non-antibacterial nature that limits its applications as safe dressing material. The deficiency prevents BC to resist against the wound infections. It is therefore of great importance to prepare BC composites with some materials that could be helpful in stopping wound infections [2]. Fibrous network structure offers an ideal scenario for *ex-situ* impregnation of nanomaterials in the internal BC matrix. Over the past decade, BC has been blended with a number of polymers and nanomaterials to prepare different composites. These composites were mainly prepared to overcome some above-listed deficiencies and increase the biological activities, physical, mechanical, conducting, magnetic properties, and biomedical applications of the BC [2,3,7]. Composites of BC with chitosan and alginates etc. have resulted in increasing the biocompatible properties of BC. BC containing Ag nanoparticle composites have revealed their promising antifungal and antibacterial properties. Similarly, BC and Au nanoparticle nanocomposite produced biomedical applications with specific uses in biosensors and enzyme immobilization processes [18]. Furthermore, BC composites with montmorillonite clay that have produced impressive antibacterial properties have been recently reported [19]. It has been observed that several shortcomings associated with pristine BC can be overcome in its composites that ultimately enhance the applications of BC.

Although antibacterial activities have been achieved successfully the goal is not what has been presented in these studies. The actual goal is to develop antibacterial BC sheets for enhanced biomedical applications. These sheets must provide protection to the healing wounds from bacterial and fungal infections during healing. But most of the previous studies have avoided that part. It must be evaluated whether these composites have any toxic effect on developing animal cells. If the toxic effect is severe than these composite hydrogels cannot be utilized as dressing materials for healing wounds. Moreover, there are other chemical compounds present in different wastewaters which causes a serious threat to human lives. Among such compounds, various pharmaceutical by-products, textile dyes, heavy metal, and chloro-, nitrophenols are the most prominent ones present in wastewater. Numerous efficient methods have been developed which have the potential to successfully eliminate such compounds from wastewater bodies to prevent or reduce its toxic effect. One such method is to use a catalyst in combination with a strong reducing agent like sodium borohydride to change the complete chemical structure of toxic organic compounds [11,15,20,21]. In fact, various metal nanoparticles such as Au, Ag, Pt, Pd, and Cu as well as some metal oxides such as CuO, copper ferrite, cobalt oxide, and others have been used as catalysts. The problem with using nanocatalysts is their recovery process. Because of extremely small nature, metal nanoparticles are difficult to be recovered from the reaction after completing it. Therefore, catalysts are nowadays deposited on some supports which helps in their easy separation. Some famous supports are the polymer fibers [16], polymer sheets (dip-catalysts) [13,22,23], magnetic nanoparticles and others [24]. BC might act as the best catalytic support because it has all those properties which are needed in a typical support material.

Herein, we report to synthesize antibacterial BC-CuO nanocomposite through a simple ex-situ synthetic strategy and will evaluate its application as a bactericidal scaffold against model pathogenic microbes. Furthermore, a threat to human lives is not only imposed by microorganism but the ever-increasing and wide usage of toxic chemicals such as nitroaromatics, heavy metals, and toxic dyes are all equally responsible [25–29]. Therefore, additional experiments of using BC-CuO as catalysts were performed on elimination and reductive degradation of Methyl Orange (MO) dye.

2. Experimental setup

2.1. Materials

The following chemicals were used within this research work, BC synthetic media consisting of glucose, peptones, acetic acid, agar, yeast extract, succinates, etc. Copper sulfate salt and sodium hydroxide base were bought from Merck. Sodium borohydride was purchased from Loba Chemie, India. Deionized water was used in all experiments. Various microbial cells including, *Acetobacter xylinus*, *Escherichia coli*, *Staphylococcus aureus* along their respective growth media were purchased from different reliable companies.

2.2. Cell growth and synthesis of BC hydrogel

BC was synthesized through a static cultivation strategy using *Gluconacetobacter* sp. cells and obtained in the form of sheets. Prior cells were grown on a basal medium containing 1.5 mL/L acetic acid, 7 g/L peptone, 10 g/L glucose, 10 g/L yeast extract, and 0.2 g/L succinate dissolved in distilled water [30]. With the inoculation of prepared cell culture, BC sheets were synthesized in specially designed reactors in 7–10 d cultivation. BC sheets were then cultivated and washed thoroughly with a 1% NaOH solution followed by heated distilled water to completely remove the cell debris and media components. Clean BC Sheets were then stored at 4°C temperature before further use. *E. coli* and *S. aureus* were used as model bacterial organisms for assessment of the prepared material's bactericidal activities. These species of bacteria were grown in the presence of prepared materials on respective culturing media for 24 h.

2.3. Synthesis of CuO

The CuO nanomaterial was synthesized following the protocol given in [31]. Two solutions of $CuSO_4$ and NaOH were prepared in deionized water with concentrations of 0.1 and 0.5 M, respectively. The NaOH solution was poured slowly into the magnetically stirring $CuSO_4$ solution and pH was monitored in the meanwhile. The addition of the NaOH solution to the CuSO4 solution was stopped upon reaching the pH to 10. The temperature of the mixed solution was raised to 80°C for the solution and the reaction was continued for 5 h. The black precipitate was obtained at the end of this reaction which was cleaned by repeated washing with ethanol and deionized water. The dried black powder was calcined at 600°C in the muffle furnace and stored for further experiments.

2.4. Preparation of bactericidal BC-CuO

BC-CuO composites were synthesized through the *ex-situ* composite synthesis strategy. Briefly, 4 cm × 4 cm BC sheets were suspended in CuO solution under the agitated condition of 200 rpm at 50°C for 24 h. The nanoparticles were allowed to attach to the BC surface and penetrate inside the BC matrix. The synthesized composites were dried and kept for further analysis.

2.5. Dry weight analysis for CuO determination in composites

The dry weight analysis of the same size of pure BC and BC-CuO composites was done to investigate the % CuO attachment to BC sheets in composites. BC sheets were cut in equal various pieces of equal size. Among those pieces, few were kept in CuO suspension for different time intervals (12, 24, 36, and 48 h) under shaking condition of 200 rpm at 50°C after treatment both composite and pure BC samples were dried and percentage of CuO penetration in BC composite was calculated from their dry weights using the following formula.

$$\text{Percent CuO} = \left(\text{Composite weight} - \text{BC weight}\right) \times 100 \quad (1)$$

Experiments were done in triplicate sets to validate the results.

2.6. Cu^{++} release studies

Stability and attachment of NP in the composite were evaluated via Ion release experiments. Freeze-dried BC-CuO composites were suspended in ethanol solution under shaking condition for different time intervals and the ion releases behavior was checked using inductively coupled plasma spectrophotometer (ICP, Thermo Jarrell Ash IRIS-AP, USA).

2.7. Characterization

Surface analyses of the bare BC and BC-CuO nanocomposites were performed by field emission–scanning electron microscopy (FE-SEM), JEOL JSM-7600F, Japan. The BC-CuO composite samples were cryo-fractured in liquid nitrogen for the detailed pore and networked structure of the BC samples. Samples were coated with platinum prior to FE-SEM analysis. The nanoparticles loaded BC hydrogel were prepared by dropping its suspension on cover glass followed by drying and coating with platinum. The instrument was operated at high KV. Photographs of the samples in the antibacterial studies were captured using Olympus Digital Camera (Japan). UV-visible spectroscopic experiments will be performed using Thermo Scientific Evolution 300, (UK), UV-visible spectrophotometer. X-ray diffraction (XRD) experiments were also performed to confirm the successful preparation of the nanoparticles and their presence in the BC-CuO composites. The instrument used was the ARL X'TRA (Thermo Scientific). Thermogravimetric analysis (TGA) was performed using a TA Instruments Q-500. Samples were heated in an inert atmosphere in the ceramic pan with a heating rate of 10°C/min.

2.8. Antibacterial activity

The antibacterial activity of the pure BC and BC-CuO was evaluated through disc diffusion assay. The selected strains include *E. coli*, a gram-negative bacterium, and gram-positive bacterium *S. aureus*. Nutrient agar (5.0 g peptic digest of animal tissue, 1.5 g beef extract, 1.5 g yeast extract, 5.0 g sodium chloride, and 15.0 g agar per liter) was used as a growth media. Agar plates were prepared, and inoculum of selected strain was spread over the media. The 20 mm discs of composite, BC, and standard drug (silver sulfadiazine) were placed over agar plates and kept at 37°C for 24 h. After which the inhibition zones were measured to determine the antimicrobial capability of nanocomposites. The experiment was replicated at least three times.

The percent inhibition was also determined by using the formula:

$$\text{Percent inhibition} = \left(\frac{\text{test sample}}{\text{standard}}\right) \times 100 \quad (2)$$

2.9. Catalyst usage

We have followed a suitable method of the dip-catalyst type reaction for the evaluation of the catalytic properties of the BC-CuO sheets [32–41]. The detailed process is described here by taking the example of MO. To proceed with the catalytic reduction of MO, its 2.5 ml of 0.1 molars aqueous solution or little condense solution was charged into a UV-cuvette. Afterward, a known amount of the BC-CuO sheet was placed inside the UV-cuvette. All changes in mixed solution color were monitored using visual observation and UV-visible spectrophotometer. After this, a reductant solution having a quite high concentration of sodium borohydride was added to the UV-cuvette to start the reduction process. The BC-CuO act as a catalyst and the reaction progress was monitored using a UV-visible spectrophotometer. The absorbance spectra were recorded continuously until the solution became completely clear. The reduction rate constants for MO was calculated by measuring the decrease in the absorption peak at λ_{max}. The λ_{max} values from the plot of a UV-Vis data were plotted against time and a suitable equation was fitted to the data to determine the rate constant of the reaction. The

reduction (%) of the dye was calculated according to the following equation:

$$\text{Reduction}\ (\%) = 100 - \left(\frac{A_t \times 100}{A_0}\right) \quad (3)$$

where A_t and A_0 indicate the absorbance value at λ_{max} at time t and before starting the catalytic reduction process (at time = zero).

3. Results and discussion

3.1. Composition and stability of composites hydrogel

The dry weight analyses of the pure BC and BC-CuO composites were done in order to find out the amount of CuO in the BC-CuO composites. The results are shown in Fig. 1a. It could be observed that particle penetration in the BC Sheet increased with time and throughout the course of treatment. However, a significant change can be seen while treating until 24 h (35%) and after that further treatment resulted in a negligible increase (39% for 48 h). These results indicate that porous BC is almost completely occupied by impregnated NPs in 24 h. Hence further treatment will not bring significant changes in composite composition owing to the unavailability of empty spaces.

The stability of synthesized composites was evaluated through Cu^{++} release studies. The release behavior studies are important for defining the composite stability as well as its toxicological estimation for potential application in wound healing [42]. High release of Cu ions could surely reduce its efficacy in medical applications. The results obtained from these studies are compiled in Fig. 1b. As indicated A very small amount of Cu^{++} was released during the course of the observation period. The released amount of Cu^{++} slowly increased with time. It reached 1.65 ppm after day 10 of incubation. Due to the slow release of the Cu^{++}, it could be confirmed that there exist strong interactions between the CuO and BC. Thus, these interactions intern the feasibility of composite for applications in medical fields.

3.2. Morphological features of synthesized composite hydrogel

FE-SEM analysis provides a notable view of particle size, shape, BC fibril arrangement, and NPs impregnation inside the BC matrix. Herein, we analyzed the morphology of synthesized nanoparticles, pure BC, and BC-CuO composite hydrogels. The results have been depicted in Fig. 2. It is clear that NPs were having roundish to oval geometry. However, the observed micrographs showed particle agglomeration that is caused during the evaporation of ethanol solvent during the drying process for SEM analysis. Therefore, better estimation regarding the particle size could be made through XRD analysis. The SEM results of pure BC indicate a fibrous structure with numerous pores of various sizes. The fibers have a net-shaped arrangement that results in high crystalline and mechanical properties of BC [30]. Besides the porous geometry provide an ideal environment for nanoparticle penetration inside the BC matrix. SEM micrographs of composite clearly indicate the attachment of NPs to the BC fibers and their deep penetration inside the BC matrix. The NPs are well distributed in the BC matrix and providing the synthesis of a homogenous composite. SEM results provide a clue for successful composites synthesis along with augmenting for higher biological features.

Fig. 3 represents the XRD patterns of the BC, CuO, and their nanocomposite. Similar to the available reports, BC exhibited three peaks in its XRD patterns. The peaks were found mostly below 2θ of 30. Specifically, the peaks were located at 2θ = 14.2°, 16.6°, and 22.4° which correspond to the crystallographic planes of (110), (110) and (200) of cellulose I, respectively. The XRD pattern of CuO nanomaterial displayed several peaks. The peak positions were at 2θ = 35.7°, 38.8°, 48°, 53°, and 58°. These peaks correspond to the (002), (111), (020) and (202) planes, respectably. No other phase of oxide of the copper or its hydroxide was detected. The XRD pattern of the BC-CuO sample consists of three peaks below 2θ = 30 and eleven peaks in the range of 2θ = 30°–80°. The peaks between the 2θ ranges of 10°–30° correspond to the BC crystals and all the peaks in the 2θ range of 30°–80° could be considered from the CuO nanomaterial based on their locations. The XRD results

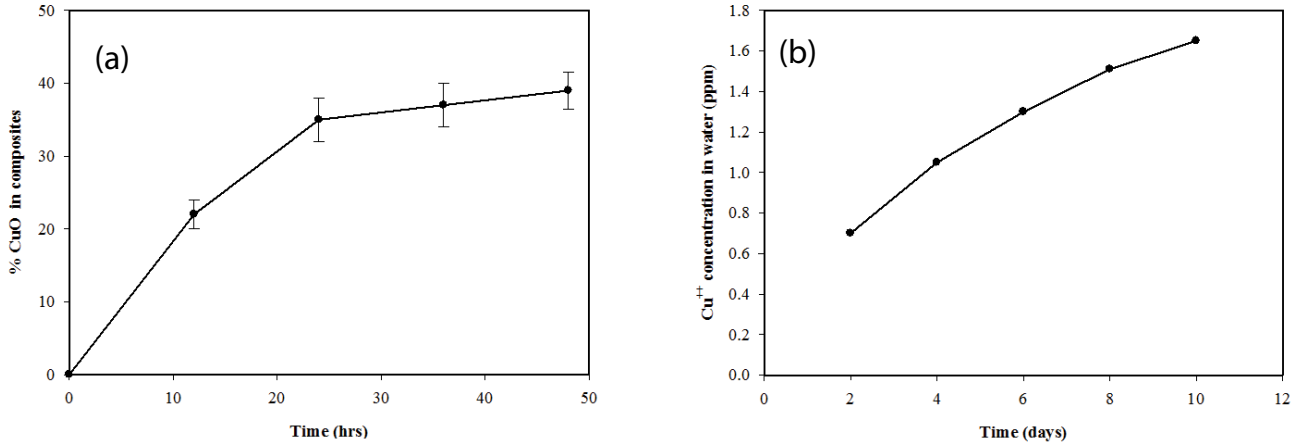

Fig. 1. (a) % composition of CuO NPs in BC-CuO composite and (b) Cu^{++} release behavior by treating BC-CuO composites in water for a different period of time.

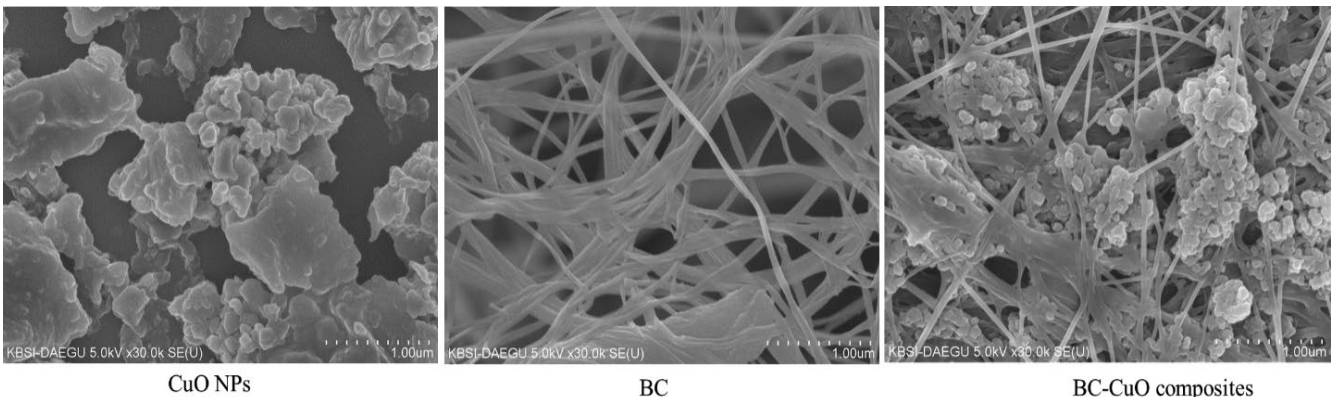

Fig. 2. FE-SEM analysis of CuO NPs, dried BC, and BC-CuO composite hydrogels.

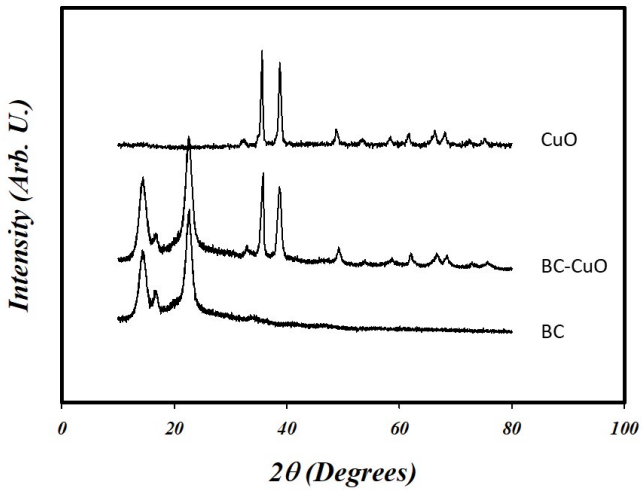

Fig. 3. XRD patterns of pure and composite samples.

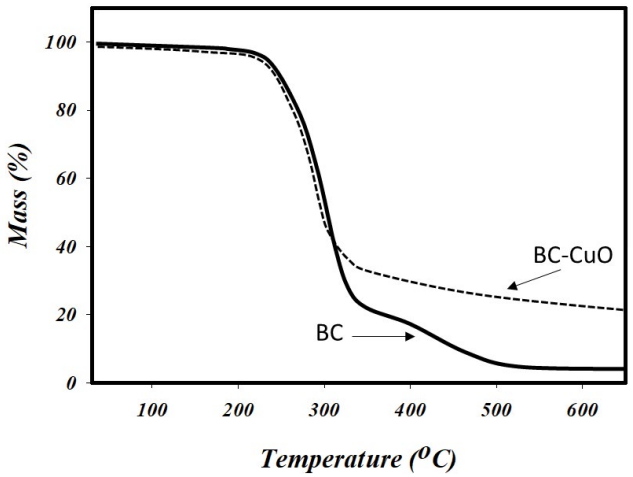

Fig. 4. TGA heating thermograms of pure BC and its composite with CuO samples.

suggest that the BC-CuO sample contained both the individual component crystals. Moreover, the broadness of the CuO peaks in both the pure form and BC-CuO sample suggest that the material was in the nano dimensions.

The TGA results of the samples are shown in Fig. 4. The thermogram of BC was similar to previously reported results. This thermogram could be divided into four sections based on slopes. In the first section, the BC material was not affected by heating treatment until the temperature reached to ~250°C as no mass reduction was observed in the thermogram. A huge mass reduction in the sample weight was observed after 250°C–340°C. This reduction was due to the degradation of the cellulose chains. Another small reduction in the weight was observed between 340°C and 520°C. It might be due to secondary degradation such as breakages of glucoside linkages and the evolution of various gases. Finally, a constant slope was obtained representing that the material was fully degraded and the only charred residue remained. In the case of the BC-CuO sample, the major transitions of weight losses were similar to the pure BC sample except for the last stage. It is clear from Fig. 4 that the remaining charred residue of the BC-CuO was more than the pure BC. This could be due to the inorganic content (CuO) in the sample which withstands with high temperature. The estimated content of the CuO in the BC-CuO sample was 17.8% which was determined from the mass values difference between the two samples at 650°C. Although this method roughly estimates the inorganic content in the polymer nanocomposite but has been widely applied as given [5,43–45].

3.3. Bactericidal activities of synthesized composites

It is an established fact that pure BC lacks antibacterial properties. This is one of the major motives for synthesizing BC composites with bactericidal materials in order to enhance its medical applications. BC composites with nanomaterials with excellent bactericidal activities have been reported [19]. Antibacterial activity of composite observed against *E. coli* (A) and *S. aureus* (B) is shown in Fig. 5. As clear from this Fig. 5, BC-CuO composites indicated effective bactericidal activities against both bacterial species. Compared to the standard drug (SD), the activities the bactericidal activities were slightly lower, as can be seen from relative inhibition zones. On the other hand, pure BC didn't show any antibacterial activity, which is in accordance with various previous reports [46]. Earlier,

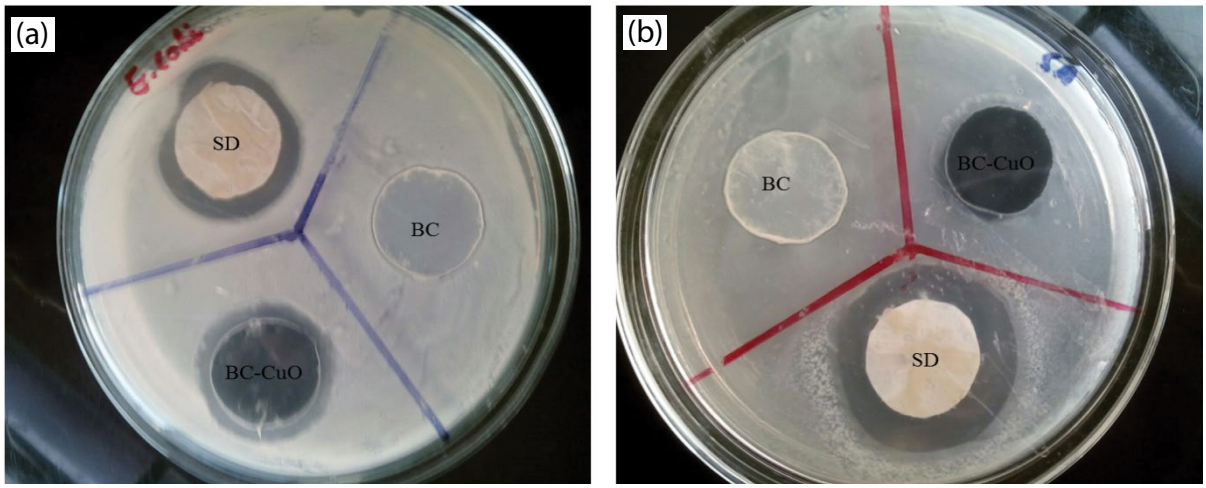

Fig. 5. Antibacterial activity of composite observed against *E. coli* (A) and *S. aureus* (B).

Zhang et al found that chitosan-CuO film restrained bacterial growth due to the inorganic component of their nanocomposite [47]. Similarly, Kouhkan et al. synthesized CuO nanoparticles using *Lactobacillus casei* subsp. *Casei* through a green route [48]. During antibacterial assays, they found that the treatment of gram-negative and gram-positive bacteria with CuO NPs inhibits the growth of these bacteria.

The total zone of inhibition and % inhibition has been shown in Table 1. The nanocomposite showed a 28 mm zone of inhibition and 96.5% inhibition when tested against *E. coli* in comparison with pure BC that does not show any activity whereas standard drug showed a 29 mm zone of inhibition. Against *S. aureus*, the nanocomposite showed 87% inhibition with a zone of 27mm as compared to pure cellulose that does not show any activity.

These results illustrate that nanoparticle impregnation inside the BC matrix gives it bactericidal features. Bactericidal features of CuO NPs are well established while the non-bactericidal nature of BC is also well known. In this scenario, the observed high bactericidal activities of composite could be attributed to the presence of CuO NPs in the BC surface and its matrix. Considering the nanoparticle release studies, it could be assumed that bactericidal effects were almost exclusively made by BC bounded NPs. This could be caused by cell membrane damage, electrostatic interaction between NPs and bacteria, or generation of reactive oxygen species. The impressive bactericidal efficacy of BC-CuO composites indicates that they can find potential applications in the pharmaceutical and biomedical fields.

Table 1
Bactericidal activities of pure BC, BC-CuO composites in comparison to standard drug

Bacterial species	Zone of inhibition (mm)			Inhibition %
	Standard drug	Pure BC	BC-CuO	
E. coli	29 ± 0	0 ± 0	28 ± 0.5	96.5
S. aureus	31 ± 0.5	0 ± 0	27 ± 1	87

3.4. MO dye reduction

Many common industries and laboratories are major sources of usage of the MO dye [14,26,29,39]. Its chemical structure is shown in Fig. 6a. As clear from its structure, it consists of an azo group due to which it is commonly named as an azo dye. Due to the azo group in its chemical structure, it is considered as toxic [37]. Many attempts have been made to change its chemical structure for the reduction of its toxicity. Among such attempts, the reduction of MO in its aqueous solution is a commonly achievable task in the presence of a reducing agent while needing an efficient catalyst. It has been well-known that several transition metals and their oxides could catalyze the reduction of MO molecules [9,23,27,28]. We test the reduction of MO dye molecules by $NaBH_4$ using the BC-CuO catalyst. In BC-CuO, the organic component of BC acts simply as a substrate while the reaction is catalyzed by CuO nanoparticles. Fig. 6b depicts the UV-Vis spectra obtained during the MO dye reduction by $NaBH_4$ while using the BC-CuO catalyst. Similar to reported literature, the UV-Vis spectrum at time zero has two absorption peaks. These peaks were located at 197 and 462 nm. The broad peak is normally used for the estimation of its concentration during reduction reactions. As the MO dye molecules reduce, the intensity of the broad peak at 462 nm decreases because the concentration of the MO dye molecules decreases. Under the current investigation, the reduction of MO dye molecules was completed in 9 min by using the BC-CuO as a catalyst because the broad peak intensity has nearly vanished. Another reaction of MO reduction by $NaBH_4$ was also carried out without using a catalyst (BC-CuO). Two more reactions were also carried out in the presence of either the synthesized pure CuO powder or a pure BC film. Fig. 6c shows the variation in reduction (%) values vs. time for the MO reduction reaction performed in the presence of the BC-CuO catalyst. Fig. 6c also shows the variation in reduction (%) values vs. time for the MO reduction reaction where no catalyst was inserted in the vessel. The variation in reduction (%) values for the MO at 462 nm for the other two reactions, where either the synthesized pure CuO powder or a pure BC film was

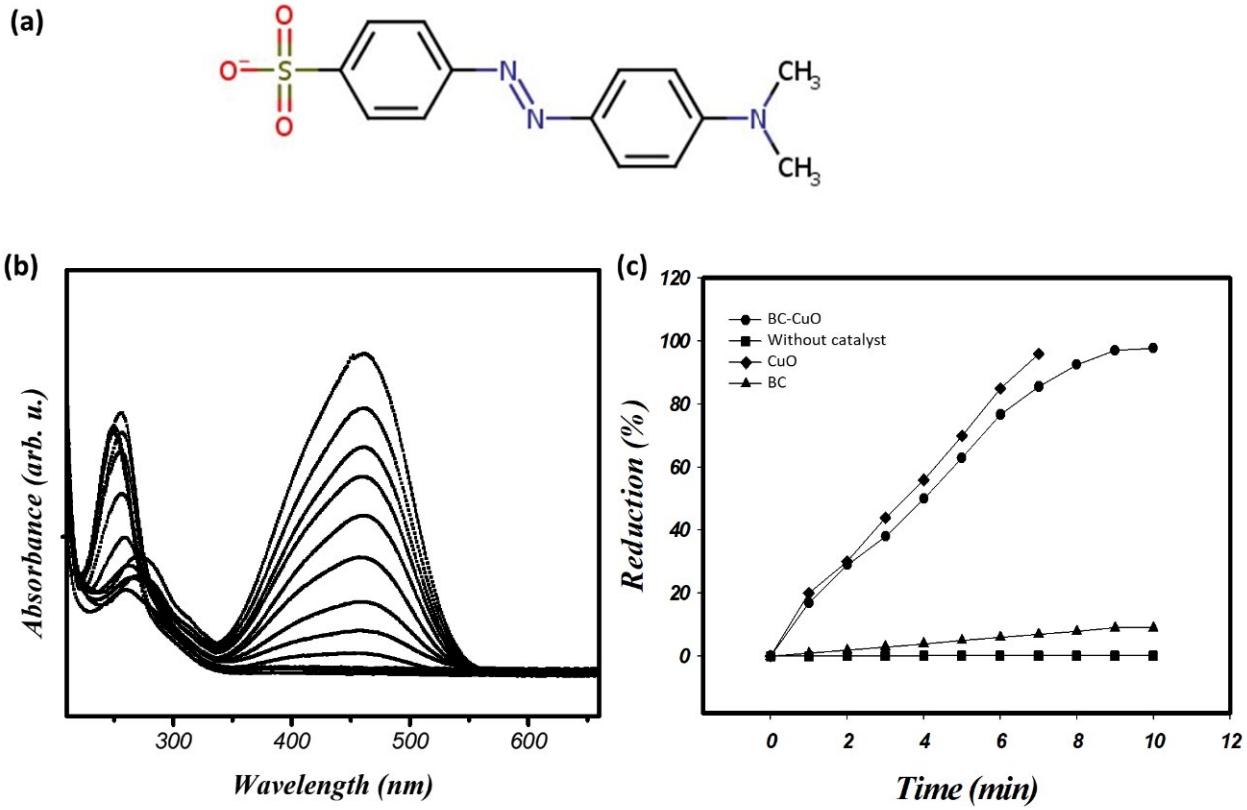

Fig. 6. Chemical structure of MO dye (a) typical absorbance spectra of MO dye catalytic reduction (b) and reduction (%) of MO dye vs. time using different substances (c).

inserted, are also shown in Fig. 6c. It can be clearly seen that reduction of the MO increased rapidly for the reaction catalyzed by BC-CuO as compared to the reaction performed without the use of a catalyst or pure BC. In both cases of CuO and BC-CuO, the reduction of the MO occurred in 10 min. Such results prove the successful part played by the BC-CuO catalyst. Fig. 7 shows the general mechanism for the MO dye reduction by $NaBH_4$ in the presence of a catalyst. The azo bond in the MO dye molecules is broken and two new molecules of small molecular weight are formed.

3.5. Reusability of BC-CuO catalyst

In chemical processing, the reusability of the heterogeneous catalyst is an important task [9,49–52]. The reusability experiments of the MO dye using the BC-CuO catalyst were performed to test its stability. In these experiments, the BC-CuO was recovered from one reaction and used immediately in another reaction as a catalyst. The reduction (%) of MO was used to check the BC-CuO activity. Table 2 lists the reusability data for the BC-CuO catalyst during its recycling process.

Table 2
MO reduction (%) by repeated reuse of BC-CuO catalyst

Entry	Cycle	Reduction (%)[a]
1	Fresh	96
2	1st reuse	90
3	2nd reuse	91
4	3rd reuse	84

[a]Values were determined after 9 min of insertion of the BC-CuO into the MO and $NaBH_4$ solution.

4. Conclusions

In this article, we synthesized CuO and BC in separate experiments and used them in their nanocomposite preparation by particle impregnation method. The morphology of the BC and CuO was examined by FE-SEM which revealed that the nanoparticles were suspended in the BC matrix and strongly adhered to the BC pellicles. XRD results showed that CuO nanomaterial was well crystalline while BC had type-I cellulose. The mixing of the two nanomaterials into BC-CuO nanocomposite had no effect on both of their crystal structures. As nanocomposite has better physical or chemical properties, we tested the antibacterial and catalytic properties of the BC-CuO. It was found that the BC-CuO had better antibacterial properties as tested against *E. coli* and *S. aureus*. Moreover, the BC-CuO played a successful role of catalyst in the MO reduction, a toxic azo, dye-containing water. The results indicate a great potential of BC-CuO as a soft reactor for the reduction of textile dyes as well as biomedical applications.

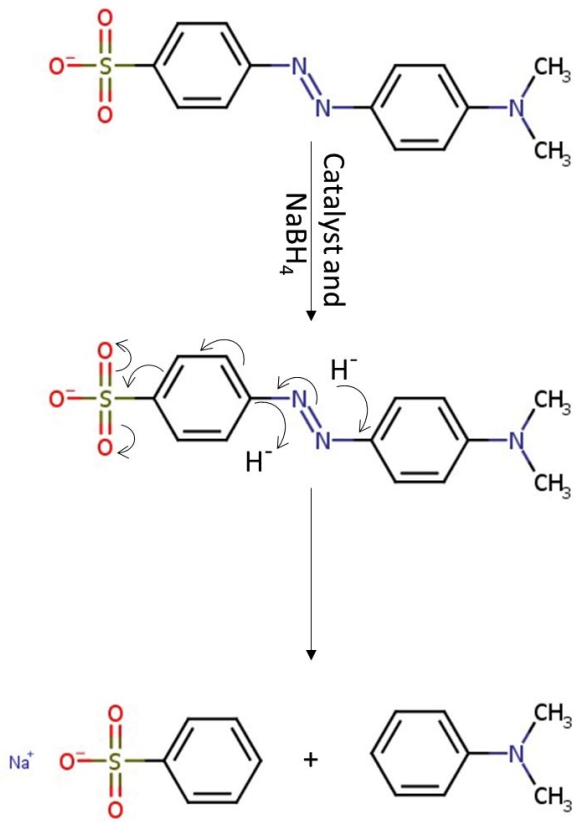

Fig. 7. Mechanism of MO dye reduction by $NaBH_4$ using the BC-CuO catalyst.

Acknowledgment

This work was supported by the Deanship of Scientific Research (DSR), King Abdulaziz University, Jeddah under grant no. (G-359-130-1440). The authors, therefore, gratefully acknowledge the DSR technical and financial support.

References

[1] M.W. Ullah, M. Ul Islam, S. Khan, N. Shah, J.K. Park, Recent advancements in bioreactions of cellular and cell-free systems: a study of bacterial cellulose as a model, Korean J. Chem. Eng., 34 (2017) 1591–1599.
[2] N. Shah, M. Ul-Islam, W.A. Khattak, J.K. Park, Overview of bacterial cellulose composites: a multipurpose advanced material, Carbohydr. Polym., 98 (2013) 1585–1598.
[3] M. Ul-Islam, S. Khan, M.W. Ullah, J.K. Park, Bacterial cellulose composites: synthetic strategies and multiple applications in bio-medical and electro-conductive fields, Biotechnol. J., 10 (2015) 1847–1861.
[4] L. Lamboni, Y. Li, J.F. Liu, G. Yang, Silk sericin-functionalized bacterial cellulose as a potential wound-healing biomaterial, Biomacromolecules, 17 (2016) 3076–3084.
[5] T. Kamal, I. Ahmad, S.B. Khan, A.M. Asiri, Bacterial cellulose as support for biopolymer stabilized catalytic cobalt nanoparticles, Int. J. Biol. Macromol., 135 (2019) 1162–1170.
[6] T. Kamal, N. Ali, A.A. Naseem, S.B. Khan, A.M. Asiri, Polymer nanocomposite membranes for antifouling nanofiltration, Recent Pat. Nanotechnol., 10 (2016) 189–201.
[7] N. Ali, Awais, T. Kamal, M. Ul-Islam, A. Khan, S.J. Shah, A. Zada, Chitosan-coated cotton cloth supported copper nanoparticles for toxic dye reduction, Int. J. Biol. Macromol., 111 (2018) 832–838.
[8] S. Khan, M. Ul-Islam, W.A. Khattak, M.W. Ullah, J.K. Park, Bacterial cellulose-titanium dioxide nanocomposites: nanostructural characteristics, antibacterial mechanism, and biocompatibility, Cellulose, 22 (2015) 565–579.
[9] F. Ali, S.B. Khan, T. Kamal, K.A. Alamry, A.M. Asiri, Chitosan-titanium oxide fibers supported zero-valent nanoparticles: highly efficient and easily retrievable catalyst for the removal of organic pollutants, Sci. Rep., 8 (2018) 6260.
[10] S.B. Khan, F. Ali, T. Kamal, Y. Anwar, A.M. Asiri, J. Seo, CuO embedded chitosan spheres as antibacterial adsorbent for dyes, Int. J. Biol. Macromol., 88 (2016) 113–119.
[11] M.S.J. Khan, S.B. Khan, T. Kamal, A.M. Asiri, Agarose biopolymer coating on polyurethane sponge as host for catalytic silver metal nanoparticles, Polym. Test., 78 (2019) 105983, doi: 10.1016/j.polymertesting.2019.105983.
[12] N. Ali, S. Azeem, A. Khan, H. Khan, T. Kamal, A.M. Asiri, Experimental studies on removal of arsenites from industrial effluents using tridodecylamine supported liquid membrane, Environ. Sci. Pollut. Res., 27 (2020) 11932–11943.
[13] I. Ahmad, T. Kamal, S.B. Khan, A.M. Asiri, An efficient and easily retrievable dip catalyst based on silver nanoparticles/chitosan-coated cellulose filter paper, Cellulose, 23 (2016) 3577–3588.
[14] I. Ahmad, S.B. Khan, T. Kamal, A.M. Asiri, Visible light activated degradation of organic pollutants using zinc-iron selenide, J. Mol. Liq., 229 (2017) 429–435.
[15] T. Kamal, I. Ahmad, S.B. Khan, A.M. Asiri, Agar hydrogel supported metal nanoparticles catalyst for pollutants degradation in water, Desal. Water Treat., 136 (2018) 290–298.
[16] T. Kamal, I. Ahmad, S.B. Khan, A.M. Asiri, Synthesis and catalytic properties of silver nanoparticles supported on porous cellulose acetate sheets and wet-spun fibers, Carbohydr. Polym., 157 (2017) 294–302.
[17] J. Dhakshinamoorthy, B. Pullithadathil, New insights towards electron transport mechanism of highly efficient *p*-type CuO(111) nanocuboids-based H_2S gas sensor, J. Phys. Chem. C, 120 (2016) 4087–4096.
[18] T.J. Zhang, W. Wang, D.Y. Zhang, X.X. Zhang, Y.R. Ma, Y.L. Zhou, L.M. Qi, Biotemplated synthesis of gold nanoparticle–bacteria cellulose nanofiber nanocomposites and their application in biosensing, Adv. Funct. Mater., 20 (2010) 1152–1160.
[19] M. Ul-Islam, T. Khan, W.A. Khattak, J.K. Park, Bacterial cellulose-MMTs nanoreinforced composite films: novel wound dressing material with antibacterial properties, Cellulose, 20 (2013) 589–596.
[20] S. Ahmed, T. Kamal, S.A. Khan, Y. Anwar, M.T. Saeed, A.M. Asiri, S.B. Khan, Assessment of anti-bacterial Ni-Al/chitosan composite spheres for adsorption assisted photo-degradation of organic pollutants, Curr. Nanosci., 12 (2016) 569–575.
[21] S.A. Khan, S.B. Khan, T. Kamal, A.M. Asiri, K. Akhtar, Recent development of chitosan nanocomposites for environmental applications, Recent Pat. Nanotechnol., 10 (2016) 181–188.
[22] E. Hariprasad, T.P. Radhakrishnan, A highly efficient and extensively reusable "dip catalyst" based on a silver-nanoparticle-embedded polymer thin film, Chem. Eur. J., 16 (2010) 14378–14384.
[23] T. Kamal, S.B. Khan, A.M. Asiri, Nickel nanoparticles-chitosan composite coated cellulose filter paper: an efficient and easily recoverable dip-catalyst for pollutants degradation, Environ. Pollut., 218 (2016) 625–633.
[24] R. Das, V.S. Sypu, H.K. Paumo, M. Bhaumik, V. Maharaj, A. Maity, Silver decorated magnetic nanocomposite (Fe_3O_4@PPy-MAA/Ag) as highly active catalyst towards reduction of 4-nitrophenol and toxic organic dyes, Appl. Catal., B, 244 (2019) 546–558.
[25] T. Kamal, Y. Anwar, S.B. Khan, M.T.S. Chani, A.M. Asiri, Dye adsorption and bactericidal properties of TiO_2/chitosan coating layer, Carbohydr. Polym., 148 (2016) 153–160.
[26] F. Ali, S.B. Khan, T. Kamal, Y. Anwar, K.A. Alamry, A.M. Asiri, Anti-bacterial chitosan/zinc phthalocyanine fibers supported metallic and bimetallic nanoparticles for the removal of organic pollutants, Carbohydr. Polym., 173 (2017) 676–689.
[27] F. Ali, S.B. Khan, T. Kamal, Y. Anwar, K.A. Alamry, A.M. Asiri, Bactericidal and catalytic performance of green nanocomposite

based-on chitosan/carbon black fiber supported monometallic and bimetallic nanoparticles, Chemosphere, 188 (2017) 588–598.
[28] F. Ali, S.B. Khan, T. Kamal, K.A. Alamry, A.M. Asiri, T.R.A. Sobahi, Chitosan coated cotton cloth supported zero-valent nanoparticles: simple but economically viable, efficient and easily retrievable catalysts, Sci. Rep., 7 (2017) 16957.
[29] F. Ali, S.B. Khan, T. Kamal, K.A. Alamry, E.M. Bakhsh, A.M. Asiri, T.R.A. Sobahi, Synthesis and characterization of metal nanoparticles templated chitosan-SiO_2 catalyst for the reduction of nitrophenols and dyes, Carbohydr. Polym., 192 (2018) 217–230.
[30] M. Ul-Islam, N. Shah, J.H. Ha, J.K. Park, Effect of chitosan penetration on physico-chemical and mechanical properties of bacterial cellulose, Korean J. Chem. Eng., 28 (2011) 1736.
[31] T. Kamal, Aminophenols formation from nitrophenols using agar biopolymer hydrogel supported CuO nanoparticles catalyst, Polym. Test., 77 (2019) 105896.
[32] M.S.J. Khan, T. Kamal, F. Ali, A.M. Asiri, S.B. Khan, Chitosan-coated polyurethane sponge supported metal nanoparticles for catalytic reduction of organic pollutants, Int. J. Biol. Macromol., 132 (2019) 772–783.
[33] T. Kavitha, S. Kumar, V. Prasad, A.M. Asiri, T. Kamal, M. Ul-Islam, NiO powder synthesized through nickel metal complex degradation for water treatment, Desal. Water Treat., 155 (2019) 216–224.
[34] A. Haider, S. Haider, I.-K. Kang, A. Kumar, M.R. Kummara, T. Kamal, S.S. Han, A novel use of cellulose based filter paper containing silver nanoparticles for its potential application as wound dressing agent, Int. J. Biol. Macromol., 108 (2018) 455–461.
[35] S. Haider, T. Kamal, S.B. Khan, M. Omer, A. Haider, F.U. Khan, A.M. Asiri, Natural polymers supported copper nanoparticles for pollutants degradation, Appl. Surf. Sci., 387 (2016) 1154–1161.
[36] N. Ali, M. Ismail, A. Khan, H. Khan, S. Haider, T. Kamal, Spectrophotometric methods for the determination of urea in real samples using silver nanoparticles by standard addition and 2nd order derivative methods, Spectrochim. Acta, Part A, 189 (2018) 110–115.
[37] T. Kamal, S.B. Khan, S. Haider, Y.G. Alghamdi, A.M. Asiri, Thin layer chitosan-coated cellulose filter paper as substrate for immobilization of catalytic cobalt nanoparticles, Int. J. Biol. Macromol., 104 (2017) 56–62.
[38] F.U. Khan, Asimullah, S.B. Khan, T. Kamal, A.M. Asiri, I.U. Khan, K. Akhtar, Novel combination of zero-valent Cu and Ag nanoparticles @ cellulose acetate nanocomposite for the reduction of 4-nitro phenol, Int. J. Biol. Macromol., 102 (2017) 868–877.
[39] S.A. Khan, S.B. Khan, T. Kamal, M. Yasir, A.M. Asiri, Antibacterial nanocomposites based on chitosan/Co-MCM as a selective and efficient adsorbent for organic dyes, Int. J. Biol. Macromol., 91 (2016) 744–751.
[40] T. Kamal, S.B. Khan, A.M. Asiri, Synthesis of zero-valent Cu nanoparticles in the chitosan coating layer on cellulose microfibers: evaluation of azo dyes catalytic reduction, Cellulose, 23 (2016) 1911–1923.
[41] T. Kamal, M. Ul-Islam, S.B. Khan, A.M. Asiri, Adsorption and photocatalyst assisted dye removal and bactericidal performance of ZnO/chitosan coating layer, Int. J. Biol. Macromol., 81 (2015) 584–590.
[42] A. Khalid, R. Khan, M. Ul-Islam, T. Khan, F. Wahid, Bacterial cellulose-zinc oxide nanocomposites as a novel dressing system for burn wounds, Carbohydr. Polym., 164 (2017) 214–221.
[43] S. Butun, N. Sahiner, A versatile hydrogel template for metal nano particle preparation and their use in catalysis, Polymer, 52 (2011) 4834–4840.
[44] S.B. Khan, S.A. Khan, H.M. Marwani, E.M. Bakhsh, Y. Anwar, T. Kamal, A.M. Asiri, K. Akhtar, Anti-bacterial PES-cellulose composite spheres: dual character toward extraction and catalytic reduction of nitrophenol, RSC Adv., 6 (2016) 110077–110090.
[45] N. Sahiner, H. Ozay, O. Ozay, N. Aktas, A soft hydrogel reactor for cobalt nanoparticle preparation and use in the reduction of nitrophenols, Appl. Catal., B, 101 (2010) 137–143.
[46] M. Ul-Islam, W.A. Khattak, M.W. Ullah, S. Khan, J.K. Park, Synthesis of regenerated bacterial cellulose-zinc oxide nanocomposite films for biomedical applications, Cellulose, 21 (2014) 433–447.
[47] Y. Zhang, H. Zhang, Y. Liu, Z.L. Zhang, C.K. Ding, Chelating ability and microbial stability of an L-arginine-modified chitosan-based environmental remediation material, J. Polym. Environ., 26 (2018) 885–894.
[48] M. Kouhkan, P. Ahangar, L.A. Babaganjeh, M. Allahyari-Devin, Biosynthesis of copper oxide nanoparticles using *Lactobacillus casei* Subsp. *Casei* and its anticancer and antibacterial activities, Curr. Nanosci., 16 (2020) 101–111.
[49] M. Ul-Islam, M.W. Ullah, S. Khan, T. Kamal, S. Ul-Islam, N. Shah, J.K. Park, Recent advancement in cellulose based nanocomposite for addressing environmental challenges, Recent Pat. Nanotechnol., 10 (2016) 169–180.
[50] T. Kamal, I. Ahmad, S.B. Khan, A.M. Asiri, Anionic polysaccharide stabilized nickel nanoparticles-coated bacterial cellulose as a highly efficient dip-catalyst for pollutants reduction, React. Funct. Polym., 145 (2019) 104395.
[51] T. Kamal, I. Ahmad, S.B. Khan, M. Ul-Islam, A.M. Asiri, Microwave assisted synthesis and carboxymethyl cellulose stabilized copper nanoparticles on bacterial cellulose nanofibers support for pollutants degradation, J. Polym. Environ., 27 (2019) 2867–2877.
[52] M. Ismail, K. Akhtar, M.I. Khan, T. Kamal, M.A. Khan, A.M. Asiri, J.C. Seo, S.B. Khan, Pollution, toxicity and carcinogenicity of organic dyes and their catalytic bio-remediation, Curr. Pharm. Des., 25 (2019) 3645–3663.